The Journal of Experimental Biology 202, 1939–1951 (1999)
Printed in Great Britain © The Company of Biologists Limited 1999
JEB1926

VOLTAGE-ACTIVATED WHOLE-CELL K^+ CURRENTS IN LAMINA CELLS OF THE DESERT LOCUST *SCHISTOCERCA GREGARIA*

CHRISTIAN BENKENSTEIN*, MANFRED SCHMIDT AND MICHAEL GEWECKE

Universität Hamburg, Zoologisches Institut, Neurophysiologie, Martin-Luther-King-Platz 3, D-20146 Hamburg, Germany

*e-mail: C_Benkenstein@public.uni-hamburg.de

Accepted 22 April; published on WWW 22 June 1999

Summary

Voltage-dependent outward currents were studied in freshly dissociated somata of locust lamina cells. These currents were recorded in 142 somata using the whole-cell patch-clamp technique. By measuring the reversal potential at altered external [K^+] and by replacing internal K^+ with Cs^+, we determined that the outward currents were carried by K^+. The outward currents consist of a transient A-type K^+ current (K_A) and a delayed-rectifier-like K^+ current (K_D). Amongst the cells studied, we observed two distinct groups of cells. The most obvious difference between the two groups is that in group I cells the total outward current is dominated by K_A (K_A/K_D=12.5), whereas in group II cells K_A makes a smaller contribution (K_A/K_D=2.1). Furthermore, in cells of group I, the K_A current shows a steeper voltage-dependence of activation, where V_{G50} is –29.9 mV and s is 11.9 (N=22), and inactivation, where V_{I50} is –84.5 mV and s is –6.3 (N=18), compared with the K_A current in cells of group II: V_{G50}=–7.9 mV; s=26.6 (N=36) and V_{I50}=–68.4 mV; s=–7.5 (N=21) (V_{G50} is the voltage at which the whole-cell conductance G is half-maximally activated, V_{I50} is the voltage of half-maximal inactivation and s is the slope of the voltage-dependence). The transient K_A current in group I cells decayed mono-exponentially. The decay of the K_A current in group II cells was fitted with a double-exponential curve and was significantly faster than in group I cells. In contrast to the large differences in K_A currents, the K_D currents appeared to be quite similar in the two groups of cells.

Key words: visual system, central nervous system, insect, electrophysiology, ion channel, K^+ current, Ca^{2+} current, locust, *Schistocerca gregaria*.

Introduction

In insects, the perception and processing of visual information has been widely studied in numerous preparations. The sensory input provided by photoreceptors located in the retina is integrated in the optic lobe by three successive neuropils: the lamina, medulla and lobula (Fig. 1A; although in flies there is an additional lobula plate; Fig. 1B shows the lamina at higher magnification). Several descending and centripetal projection neurons of insects have been characterized in terms of their morphology and electrophysiological responses to visual stimuli (e.g. O'Shea et al., 1974; Stavenga and Hardie, 1989; Rind, 1990a,b; Gewecke and Hou, 1993), and the functional properties of optic lobe neurons have been studied by analysing ligand- and voltage-activated currents in lamina monopolar cells (LMCs) located in the lamina. The LMCs are postsynaptic to the photoreceptors and thus represent the first level of signal processing in the visual pathway. Recordings from these cells have been made using whole-cell and single-channel patch-clamp techniques to characterize histamine-activated Cl^- channels and voltage-activated K^+ channels (Hardie, 1987, 1988; Hardie and Weckström, 1990; Skingsley et al., 1995). However, investigations of LMCs have been restricted to flies, with the exception of a study of lamina neurons from locusts carried out by Schmidt et al. (1998).

Various immunocytochemical studies suggest that not only neurotransmitters but also neuromodulators, such as biogenic amines and neuropeptides, play a role in signal processing in the central nervous system (CNS) of insects (for reviews, see Nässel, 1991; Homberg, 1994). The possibility that central modulation of sensory processing also occurs in the optic lobe is suggested by the presence of a small group of octopaminergic centrifugal brain neurons (PM neurons) in locusts, which project from the protocerebrum to the medulla, where they show extensive arborizations (Stern et al., 1995). Bacon et al. (1995) showed that octopamine released by these PM neurons is responsible for dishabituation of the giant descending contralateral movement detector (DCMD) neuron arborizing in the optic lobe of locusts. Furthermore, Hevers and Hardie (1995) have shown that *Shaker* and delayed-rectifier channels in *Drosophila melanogaster* photoreceptors are affected by serotonergic modulation.

In this study, we focus on the kinetic and pharmacological properties of voltage-activated K^+ currents in freshly dissociated lamina neurons of desert locusts. To obtain data

comparable with those from the LMCs of flies, Schmidt et al. (1998) developed a technique to obtain stable whole-cell patch-clamp recordings from freshly dissociated lamina neurons. Freshly dissociated somata have the advantage that possible artefacts induced by primary culture conditions are excluded and thus that the cells are more likely to show the same properties as those existing *in situ*. This technique has been used in the present paper and will be employed in future experiments on the effects of biogenic amines and other putative modulators on the voltage-activated currents in lamina neurons.

Materials and methods

Animals

We used approximately 35 young adult desert locusts (*Schistocerca gregaria* Forskål) of both sexes 3–5 days after their imaginal moult. The locusts were reared in a crowded colony under constant conditions. They were kept at approximately 35 °C on a 12 h:12 h light:dark cycle on a diet of grass and carrots.

Dissection and preparation of cells

The animals were decapitated, the head was pinned in a dissecting dish, and the entire brain, including the retinas, was removed from the head capsule. Under normal locust saline (see Solutions), the retinas were removed and the optic lobes carefully desheathed. After an enzyme treatment with 1‰ papain solution (Boehringer) and 3 mg of cysteine in 1 ml of locust saline for 10–15 min (depending on room temperature, which varied between 20 and 25 °C), the optic lobes were rinsed for 20–30 min in locust saline. Subsequently, somata of the lamina cells were obtained by 'dabbing' the distal surface of the lobes onto the bottom of the recording chamber (Fig. 1C). To ensure that only lamina neurons were recorded, we selected somata of 12±1 μm in diameter located in the centre of the fields of somata obtained by dabbing the distal side of the lamina (Fig. 1D). According to Nowel and Shelton (1981) and Schmidt et al. (1998), somata of LMCs do not exceed 17 μm in diameter.

The recording chamber consisted of a Perspex ring (inner diameter 12 mm; height 3 mm; volume approximately 0.3 ml) fixed onto a fresh plastic dish (Falcon) for each experiment using a thin layer of petroleum jelly. On the stage of an inverted microscope (precision inverted microscope; World Precision Instruments), the recording chamber was continuously perfused with fresh locust saline at approximately 3 ml min^{-1} (except during the application of voltage-step protocols, when perfusion was discontinued to avoid capacitative errors due to changing fluid levels in the chamber). Using solenoids and various application tubes, switching between normal saline and saline containing blocking agents was possible. A complete exchange of the bath contents was achieved within 60 s. The K^+ channel blockers $BaCl_2$, CsCl, tetraethylammonium (TEA^+), 4-aminopyridine (4-AP) and quinidine were applied extracellularly at concentrations of 10 mmol l^{-1} or 50 μmol l^{-1} (quinidine).

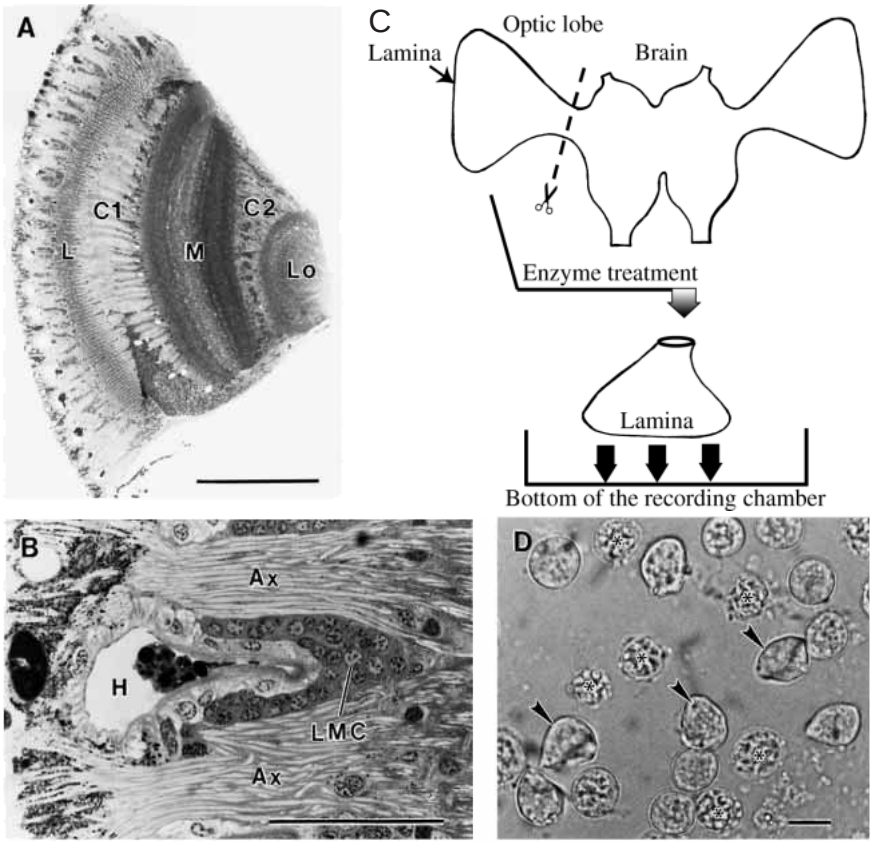

Fig. 1. Morphology of the optic lobe and of the dissociated somata of lamina neurons with a diagram to illustrate the preparation of lamina neurons. (A) Horizontal section through the optic lobe showing the lamina (L), medulla (M), lobula (Lo) and the two optic chiasmata (C1, C2); stained with Methylene Blue. Scale bar, 500 μm. (B) Lamina at higher magnification with somata of lamina monopolar cells (LMC), descending axons of the photoreceptors (Ax) and a haemolymph channel (H). Scale bar, 100 μm. (C) The preparation of freshly dissociated somata of lamina neurons. The severed optic lobe is desheathed, treated with papain and subsequently dabbed with its distal surface onto the bottom of a tissue culture dish. (D) Freshly dissociated somata of lamina neurons adhering onto the bottom of the recording chamber. Cells chosen for recording were those without a heavily granular cytoplasm and with a clearly discernible cell membrane (arrowheads). Cells with granular cytoplasm (asterisks) were excluded from recording. Scale bar, 10 μm.

Patch-clamp recordings

Whole-cell gigaohm seal recordings were performed at room temperature (20–25 °C) according to the method of Hamill et al. (1981). Electrodes were prepared on a Narishige PC-10 vertical puller. We used thick-walled borosilicate glass capillaries (GB150-8P; Science Products) with a bubble number of 5.4–5.8 (Mittman et al., 1987) and a resistance of approximately 4–5.5 MΩ in normal locust saline (see Solutions). Electrodes pulled immediately before use and not fire-polished yielded the best results.

An EPC9 patch-clamp amplifier (HEKA) was used in combination with the appropriate hard- and software equipment (Pulse, HEKA) running on a Pentium PC for stimulus generation, storage and analysis of data. The pipette capacitance ranged from 8 to 11 pF and was compensated prior to recording from the cell. The membrane capacitance (3.56±0.95 pF, mean ± S.D., N=115) was compensated before each sweep of a voltage-step protocol. The series resistance (23.63±14.21 MΩ, mean ± S.D.; N=126) was compensated by 75–80 %. The remaining error of 20–25 % uncompensated series resistance will have caused a mean deviation in command potential of less than 5.9 mV per nA of whole-cell current. Since some of the cells showed whole-cell currents of 8–10 nA, the resulting voltage error was up to 60 mV. The currents were two-stage filtered with a three-pole Bessel filter at 10 kHz and a four-pole Bessel filter at 3.1 kHz in series. The data were digitally sampled at 10 kHz. The liquid junction potentials between bath and pipette solution were measured according to the method of Neher (1992). Liquid junction potentials and leakage currents were corrected online.

Statistics

The statistical analysis required for cell classification was performed using SPSS 6.3. For the hierarchical cluster analysis, we used Ward's method. The squared euclidic distance was taken as a measure of proximity between analyzed cells. Other statistical calculations were performed in PSI-Plot (Poly Software International).

Solutions

The bath was perfused with normal locust saline as the standard external solution (in mmol l^{-1}): 200 NaCl, 5 KCl, 3 $MgCl_2$, pH 7.0 with 10 mmol l^{-1} Hepes/NaOH. For experiments to establish reversal potential and rectification, the K^+ concentration was altered to 50, 100 or 185 mmol l^{-1}. The osmolarity was always kept at 400 mosmol l^{-1} by reducing the NaCl concentration accordingly. The various K^+ channel blockers were added to this solution at the concentrations noted above. In the case of 4-AP, additional pH adjustment was necessary. The standard internal solution consisted of (in mmol l^{-1}): 180 potassium gluconate, 5 KCl, 10 NaCl, 2 $MgCl_2$, 1 $CaCl_2$, 10 EGTA, pH 7.0 with 10 mmol l^{-1} Hepes/KOH. $BaCl_2$, 4-AP and potassium gluconate were obtained from Merck; all other chemicals were purchased from Sigma.

Results

General properties of lamina cells

Dabbing the distal surface of the optic lobe onto a culture dish typically yielded large fields of adherent cells. Cells inside these fields were very similar in terms of diameter and shape. From these, somata with a diameter of 12±1 μm were selected for the recordings (Fig. 1D). Sometimes small clusters of cells also adhered but, since their identity was uncertain, these cells were excluded from recording. Most of the recorded neurons were spherical, although some had processes 5–12 μm long. Using localized dabbing and subsequent size selection, we aimed at recording primarily from lamina monopolar cells (LMCs), whose somata are localized at the distal surface of the lamina and do not exceed 17 μm in diameter (Fig. 1B). The input resistance of the lamina cells was 4.4±0.1 GΩ (mean ± S.D., N=25) calculated from the current elicited by a hyperpolarizing voltage step to −100 mV. The capacitance of the cell bodies, determined by the capacitance compensation of the amplifier, was 3.6±0.9 pF (mean ± S.D., N=115). The resting potential measured immediately after breaking into the cell was −37±7.9 mV (mean ± S.D., N=13) in group I cells (cells with peak K_A currents from 4 to 12 nA), whereas cells of group II (cells with peak K_A currents ⩽2 nA) had a more positive resting potential of −22.6±6.1 mV (mean ± S.D., N=19). The difference in resting potential was statistically significant (t-test: P⩽0.01). The cells could be held in the whole-cell recording configuration for up to 30 min.

Voltage-activated K^+ currents

We recorded from 142 neuronal somata freshly dissociated from the lamina of the locust optic lobe. All recorded somata showed voltage-activated currents. Under standard ionic conditions, only outward currents were present (Fig. 2A). In four out of eight cells recorded with 10 mmol l^{-1} $BaCl_2$ in the bath, an inward current could also be detected. We then carried out experiments to determine whether the outward currents were carried by K^+. After partially replacing external Na^+ with equimolar amounts of K^+, inward K^+ currents were observed, as was to be expected in the presence of an increased $[K^+]_o$. Recordings with a symmetrical K^+ concentration indicated outward rectification (Fig. 2B,C). The reversal potential for each $[K^+]_o$ was determined on the basis of tail currents elicited by an appropriate voltage protocol (see the inset of Fig. 2D) (Fig. 2D,E). For each $[K^+]_o$, the mean reversal potential (N=3) was plotted against the K^+ concentration (in mmol l^{-1}) (Fig. 2F). Averaged measured values are: $[K^+]_o$=5 mmol l^{-1}, E_{rev}=−82.4±8.2 mV (mean ± S.D.); $[K^+]_o$=50 mmol l^{-1}, E_{rev}=−34.4±1.8 mV; $[K^+]_o$=100 mmol l^{-1}, E_{rev}=−12.3±1.5 mV; and $[K^+]_o$=185 mmol l^{-1}, E_{rev}=−0.9±2.9 mV. Except at 5 mmol l^{-1} $[K^+]_o$, these values matched well with the respective values calculated from the Nernst equation (r^2=0.81, P=0.098). The deviation at 5 mmol l^{-1} $[K^+]_o$ may be due to the outward rectification of the K^+ currents. Replacing the internal K^+ with equimolar Cs^+ eliminated or dramatically reduced the voltage-activated outward currents (Fig. 2G). Since it is known that the

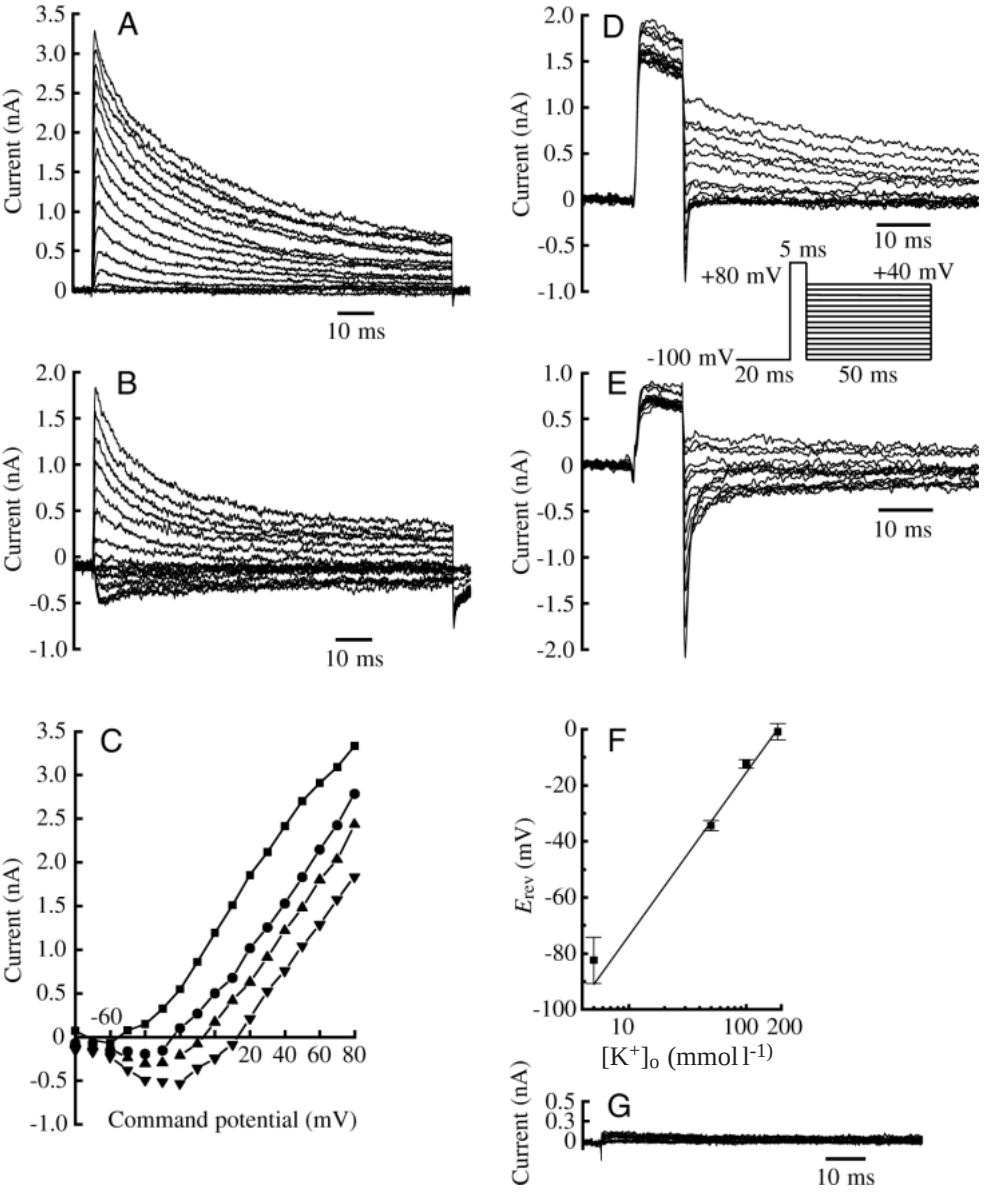

Fig. 2. Voltage-activated whole-cell K^+ currents recorded from somata of lamina neurons of the optic lobe. (A) K^+ outward currents (external solution with $[K^+]_o$=5 mmol l^{-1}, 0 mmol l^{-1} Ca^{2+}) obtained by stepping to depolarizing potentials (from –60 to +80 mV for 50 ms) after a 100 ms long prepulse of –120 mV to remove the inactivation. (B) Whole-cell K^+ currents recorded as in A in symmetrical $[K^+]$ of 185 mmol l^{-1}. Note the inward K^+ current. (C) Current–voltage relationships obtained by plotting the peak transient current *versus* the command potential for various external K^+ concentrations: ■ 5 mmol l^{-1} $[K^+]_o$, ● 50 mmol l^{-1} $[K^+]_o$, ▲ 100 mmol l^{-1} $[K^+]_o$ and ▼ 185 mmol l^{-1} $[K^+]_o$. Inward K^+ currents increase with increasing external K^+ concentration. (D,E) Tail currents obtained by the tail protocol as shown in the inset below D recorded with 5 mmol l^{-1} $[K^+]_o$ (D) and 185 mmol l^{-1} $[K^+]_o$ (E). (F) Plot of reversal potential (E_{rev}) (mean ± S.D.) at each $[K^+]_o$ as determined from tail currents (N=3) *versus* the external $[K^+]_o$. Mean measured values are: $[K^+]_o$=5 mmol l^{-1}, E_{rev}= –82.4±8.2 mV (mean ± S.D.); $[K^+]_o$= 50 mmol l^{-1}, E_{rev}=–34.4±1.8 mV; $[K^+]_o$=100 mmol l^{-1}, E_{rev}=–12.3±1.5 mV; $[K^+]_o$=185 mmol l^{-1}; E_{rev}=–0.9±2.9 mV (r^2=0.81, P=0.098). The solid line represents the theoretically expected values as calculated from the Nernst equation. (G) Outward currents recorded in normal saline after replacing internal K^+ with equimolar Cs^+. Only extremely small outward currents could be evoked, showing that the outward currents present with normal $[K^+]_i$ are carried by K^+.

permeability of Cs^+ through K^+ channels is very low (relative permeation rate ⩽0.14; Hille, 1992; p. 352), this confirms that the outward currents are carried by K^+.

In the majority of somata (93 %), at least two types of outward current were present. One of these was a rapidly activating and inactivating transient current, which can be activated only after a certain period of hyperpolarization. In this study, we will refer to this current as the K_A current, according to Hille (1992). We measured this K_A current within the first 15 ms of the voltage step. The second type of current activated significantly more slowly and showed little or no inactivation during the voltage step. This current was measured within the last 20 ms of the test pulse. We will refer to this delayed-rectifier-like current as the K_D current (see Fig. 4B,E).

To separate the two types of currents, we used a combination of two different voltage-step protocols. A voltage-step protocol with strongly hyperpolarizing prepulses (–120 mV, 100 ms) to remove the inactivation of the fast K_A current was used to record the sum of the two current components (the activation of the K_D current is not affected by the hyperpolarizing prepulses). The K_D current was specifically elicited by a voltage step protocol with a depolarizing prepulse of –30 mV (100 ms). The K_A current was then determined by subtracting the K_D current from the total current.

For 80 cells chosen randomly out of the 142 recorded, current/voltage (I/V) curves for the isolated K_A current were plotted (Fig. 3). Although all recordings are from cells of roughly the same size, the peak current elicited by a strongly depolarizing voltage step to +80 mV varied considerably (from 0.28 to 12.3 nA) between cells. With respect to the peak

currents, the cells represented in Fig. 3 can be divided roughly in two groups, which we have called group I and group II. Group I comprises cells with a peak K_A current in the range 4–12 nA; cells of group II have peak K_A currents not exceeding 2 nA.

To test the validity of the preliminary division of these cells into two different groups, we performed a cluster analysis and a subsequent discrimination analysis using the software SPSS. This analysis was based on a set of nine different variables extracted from the K_A and K_D currents measured in each cell (N=96): τ_1, the membrane time constant of the first, rapidly inactivating component of the K_A current; I_{KApeak}, the peak K_A current (measured at +80 mV); I_{KDpeak}, the peak K_D current (measured at +80 mV); I_{KA}/I_{KD}, the ratio of the peak K_A to the peak K_D current; V_{G50}, the voltage of half-activation of the K_A current and its corresponding slope factor s; V_{I50}, the voltage of half-inactivation of the K_A current and its corresponding slope factor s; $I_{K\text{-}30}$, the outward current upon a prepulse of –30 mV.

To determine the crucial variables for a division into different groups of cells, we first performed a cluster analysis. This showed that the decisive variable for a division into two groups was $I_{K\text{-}30}$. On the basis of this variable, the cells were placed into group I or group II. All the cells in group I (N=22) showed an outward current elicited by a depolarizing prepulse to –30 mV, while the remaining cells lacked such a current. A discrimination analysis excluding $I_{K\text{-}30}$ showed that the remaining variables were also sufficient for a significant separation. In this analysis, the variables s for V_{G50} and I_{KApeak} were most decisive. On the basis of these two variables, 36 cells could be attributed to group II. The remaining 38 cells could not be grouped significantly. The outward currents of a typical member of a cell of each group are depicted in Fig. 4A–F.

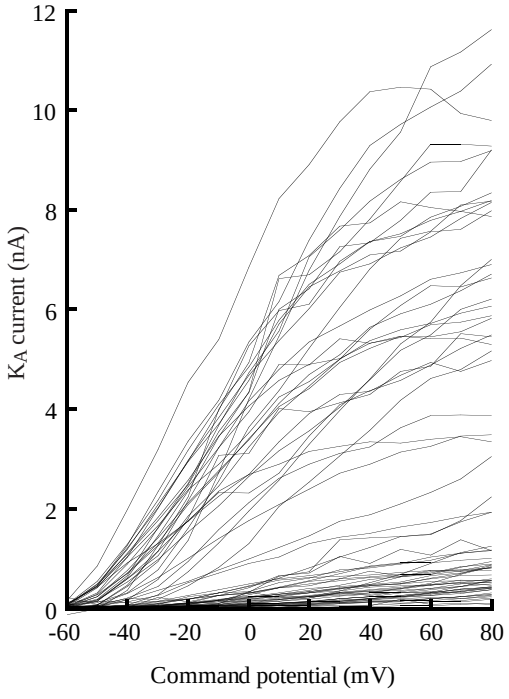

Fig. 3. The current/voltage relationships of 80 cells chosen randomly from 142 cells. The peak K_A currents measured in zero-[Ca^{2+}] saline were plotted against the command potential. The cells fall into two groups, one group with peak currents in the range 4–12 nA and with a threshold of activation of approximately –60 mV (group I), and a second group with peak currents below 2 nA activating above –40 mV (group II).

Voltage-dependence of activation of K_A and K_D currents

For the K_A and K_D currents of both groups of cells, the voltage-dependence of activation was determined in the following way: the chord conductances (G) were calculated from the measured I/V relationships according to:

$$G = I/(V - E)\,, \tag{1}$$

in which I is the measured peak current at a given command potential V, and E is the measured mean reversal potential of –82.4 mV.

The values were normalized and plotted as a function of the command potential (Fig. 5A,B). The resulting curve was fitted by a modified Boltzmann distribution of the form:

$$G/G_{max} = 1/\{1 + \exp[(V_{G50} - V)/s]\}\,, \tag{2}$$

where G/G_{max} is the normalized conductance, V_{G50} is the potential at which half the conductance is activated, and the slope factor s (mV) is a constant describing the voltage-dependence. Often the conductance curves were not sigmoidal (see Fig. 5C,D) with a steady state at the end. To obtain reliable and accurate values for V_{G50} and s in these cases, we used another modified Boltzmann equation:

$$G/G_{max} = g(1/\{1 + \exp[(V_{G50} - V)/s]\})\,, \tag{3}$$

in which g is a multiplication factor in the range of G_{max}. Measured at a depolarizing membrane potential of +80 mV, cells in group I showed a peak K_A current of 8.4±1.9 nA (mean ± S.D., N=21); the peak K_D current measured at the same potential was 0.72±0.23 nA (mean ± S.D.). The mean I_{KA}/I_{KD} ratio is 12.5±3.5 (mean ± S.D.), showing that the voltage-activated currents of group I cells are dominated by K_A. For the cells in this group, V_{G50} was –29.9 mV for K_A and –20.5 mV for K_D. The activation curve for K_A (Fig. 5A) is significantly steeper (s=11.9) (P=0.03, r^2=0.94) than that for K_D (s=20.4; Fig. 5B) (P=0.02, r^2=0.98). The peak whole-cell conductances for K_A elicited around +20 mV were in the range 30–90 nS, while the peak conductances for K_D around +40 mV ranged from 2.5 to 7.5 nS.

In group II cells, the peak K_A current is 0.92±0.4 nA (mean ± S.D., N=18) and the peak K_D current is 0.5±0.32 nA (mean ± S.D.). This results in a mean I_{KA}/I_{KD} ratio of 2.12±1 (mean ± S.D.), indicating that in group II cells K_A and K_D both contributed significantly to the total voltage-activated currents. In these cells, the conductance is half-activated at –7.9 mV for K_A, with a corresponding slope factor s of 26.6 (P=0.02, r^2=0.93) (Fig. 5C). In contrast to the cells in group I, V_{G50} for K_D is only slightly more positive, with a value of –7.4 mV. The

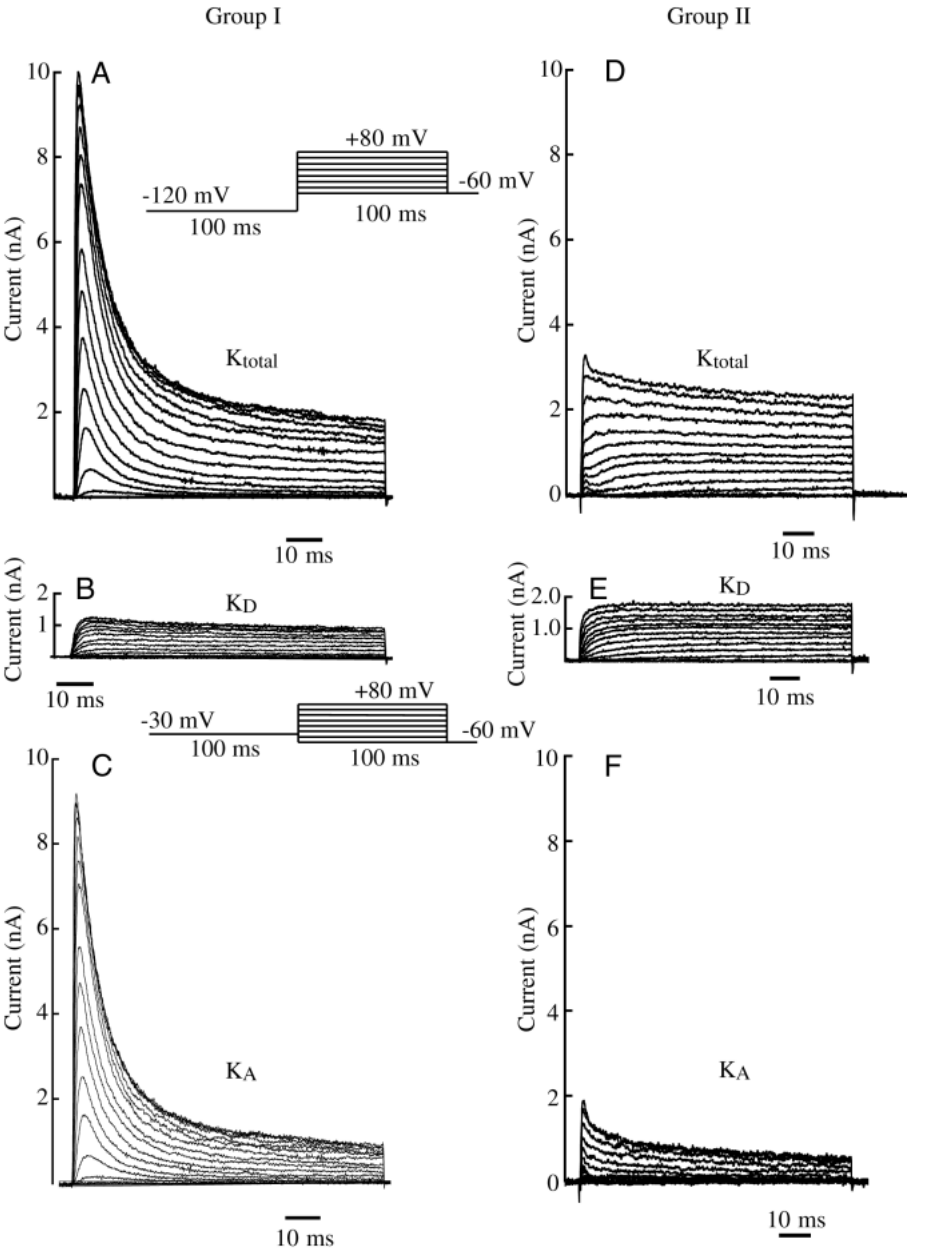

Fig. 4. A comparison between voltage-activated K^+ currents of a typical group I cell (A–C) and a typical group II cell (D–F). (A,D) Total K^+ currents (K_{total}) recorded using a step protocol (shown as an inset in A) with a strongly hyperpolarizing prepulse of −120 mV. (B,E) K_D currents recorded using a step protocol with a depolarizing prepulse to −30 mV (shown as an inset below B). (C,F) K_A currents obtained by subtraction of K_D from the total current (A minus B, D minus E). Note that the cell groups differ mainly in the peak relative contribution of the K_A current to the total current, whereas the K_D current is similar. In both cell types, the K_A current shows a late component that does not inactivate during the voltage step.

slope factor *s* of 16.2 indicates that, in this case, the voltage-dependence is steeper for K_D (P=0.051, r^2=0.98) (Fig. 5D). The peak conductances for K_A and K_D showed their maxima at +80 mV (K_A, 2–12 nS; K_D, 1–6.5 nS).

Kinetics and voltage-dependence of inactivation of K_A and K_D currents

The voltage-dependence and kinetics of inactivation were analyzed only for the K_A currents since the K_D currents of the recorded cells show little or no inactivation during a 100 ms voltage step. We generated steady-state inactivation curves for the K_A currents of cells from both groups by applying voltage steps to a constant activating potential of +60 mV (100 ms) after a 500 ms long conditioning prepulse ranging from −100 mV to +20 mV in 10 mV increments and measured the peak current elicited by the activating test pulse. For each trace, the K_D current (measured at the end of the test pulse) was subtracted from the total current to obtain the K_A current. The averaged normalized steady-state inactivation curves are depicted in Fig. 6A,C and were fitted with equation 2. For the cells in group I (N=18), this fit yielded a half-inactivation voltage (V_{I50}) of −84.5 mV and a slope value *s* of −6.3 mV (Fig. 6A). The cells of group II show a mean V_{I50} value of −68.4 mV and a slope factor *s* of −7.5 mV (Fig. 6C). While the K_A currents of cells of group I cells are totally inactivated at a prepulse potential of −40 mV, in cells of group II a 30–35 % activation of K_A currents remains at more depolarizing potentials in the range −40 to +20 mV.

For both groups of cells, we determined the time constant of inactivation τ_1 of the K_A currents. For this purpose, we

analyzed the peak K_A currents elicited by a conditioning prepulse (−120 mV; 100 ms) followed by a depolarizing test pulse (100 ms) to +80 mV. We have chosen to analyse the peak current traces since smaller amplitudes could not often be fitted properly. The decay of the evoked peak currents was fitted with a single-exponential or, if necessary, with a double-exponential function of the form:

$$I(t) = A_0 + A_1\exp(-t/\tau_1), \quad (4)$$

$$I(t) = A_0 + A_1\exp(-t/\tau_1) + A_2\exp(-t/\tau_2), \quad (5)$$

where A_0 is the activating component of the current, A_1 is the first, rapidly inactivating component of the current, A_2 is the more slowly inactivating component of the current, t is time and τ is the membrane time constant of inactivation. Irrespective of the grouping, K_A currents of all cells showed a non-inactivating current component A_2 at the end of the test pulse. A pulse duration of 100 ms is too short to achieve accurate values for τ_2, the time constant of inactivation for the non-inactivating current component A_2. Only the values for τ_1 describing the rapidly inactivating current component A_1 were determined. The time constants τ_1 for cells in group I are significantly (t-test: $P \leqslant 0.01$) larger (12.3±7.9 ms, N=21) than those for cells in group II (4±3.9 ms) (N=32). This means that, in cells of group I, K_A (Fig. 6A,B) decayed much more slowly than in cells of group II (Fig. 6C,D). A summary of these data is given in Table 1.

Pharmacology of K_A and K_D currents

In addition to using distinct voltage-step protocols to isolate the different K^+ currents, we employed several blocking agents to reveal differences in their pharmacological profiles. We found that 4-AP blocked mainly the K_A current, whereas quinidine and TEA^+ predominantly blocked the K_D current. $BaCl_2$ reduced both currents equally, while CsCl, applied externally, had only a small, statistically insignificant blocking effect on the currents examined in this study. Owing to the small number of cells investigated, the data for recovery after CsCl treatment were not evaluated.

In Table 2 the mean reduction of the K_A and K_D currents

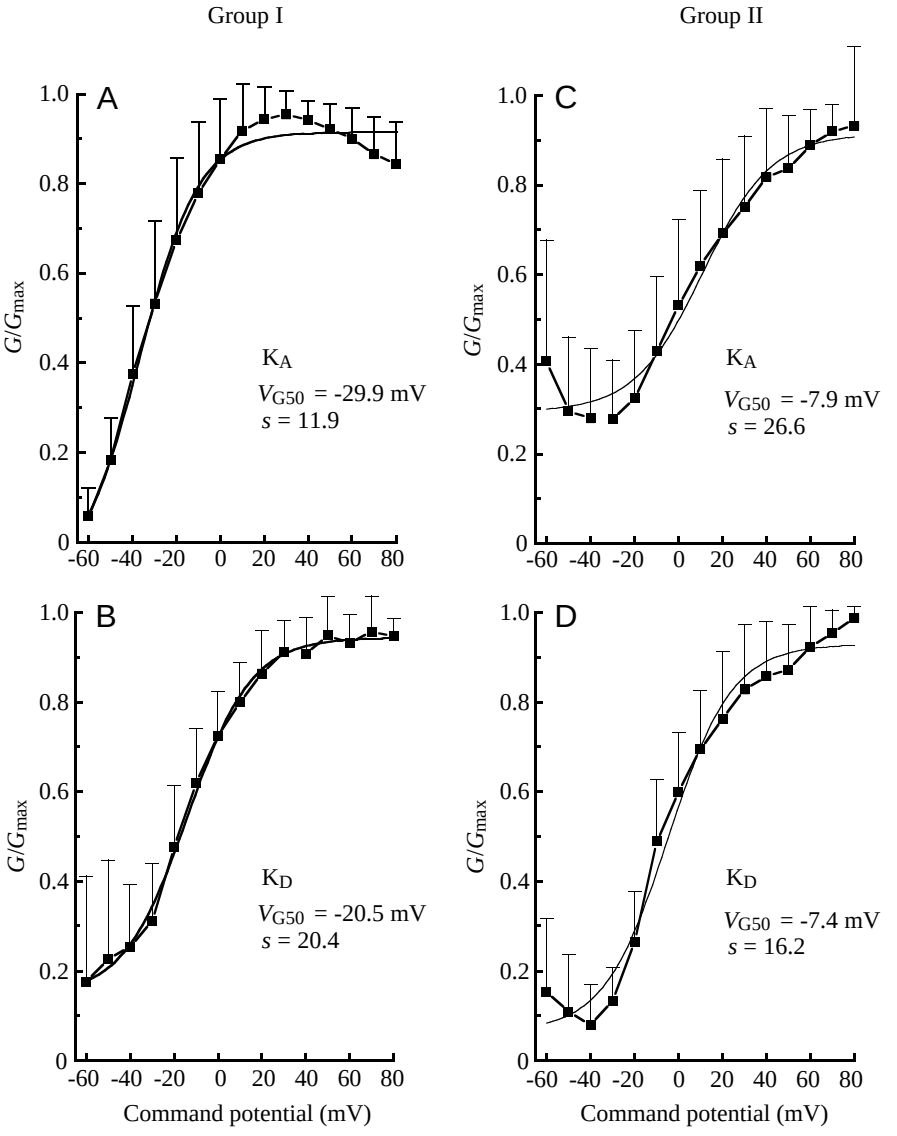

Fig. 5. Voltage-dependence of activation in cells of group I (N=22) and group II (N=36). In each case, the normalized conductance (G/G_{max}) is plotted against the command potential (mean ± S.D.) and fitted by a Boltzmann distribution (equation 2; thin line). (A) The K_A current in group I cells operates at significantly more negative potentials (t-test: P<0.01) in common with a significantly steeper voltage-dependence (t-test: P<0.01) than does the K_A current of group II (C). (B) The K_D current of group I cells also has its midpoint of activation at significantly more negative potentials (t-test: P<0.01) than the K_D current of group II cells (D). (B,D) The two K_D currents show only small differences in their voltage-dependence. The curves of group II cells were fitted using equation 3. The negative slope region at command potentials between −60 mV and −40 mV is presumably an artefact caused by conversion of small current values into normalized conduction values (C,D). G/G_{max}, normalized conductance; V_{G50}, voltage at which half the conductance is activated; s, slope of the voltage-dependence.

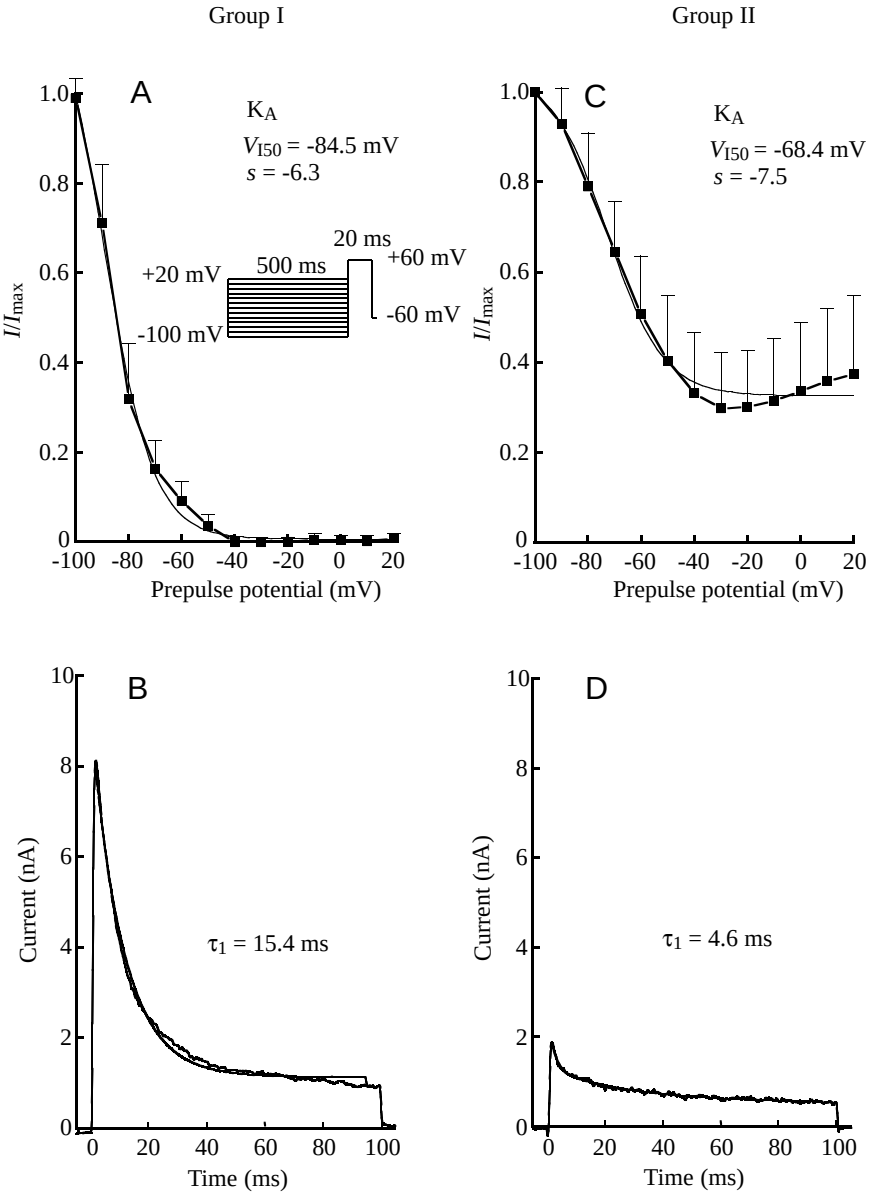

Fig. 6. Steady-state inactivation and kinetic properties of the K_A current in cells of group I (A,B) and group II (C,D). Steady-state inactivation curves were generated from the normalized and averaged peak currents (means ± S.D.) and fitted with the modified Boltzmann equation. The K_D current has been subtracted from each trace of the total current to obtain a better estimate of the K_A current. (A) The K_A current of group I cells (N=18) is half-inactivated significantly closer to the reversal potential (t-test: P<0.01) and shows a significantly steeper voltage-dependence of inactivation (t-test: P<0.01) than the K_A current of group II cells (N=21) (C). In the K_A current of group II cells (C), a non-inactivating current component (30–35 %) remains at prepulse potentials from –40 to +20 mV. (B,D) The peak current traces of the isolated K_A current (K_{total} minus K_D) are fitted to determine the membrane time constant τ_1 for the inactivation of the fast current component. (B) For a cell of group I, the curve was fitted (thin line) with a single-exponential function (equation 3) and yielded a τ_1 of 15.4 ms. (D) The current elicited in a cell of group II is fitted by a double-exponential function (equation 4; the thin line marking this is almost invisible since it is congruent with the plotted data). The resulting τ_1 is 4.6 ms, indicating a more rapid inactivation of the fast current component than in the cell of group I. I/I_{max}, normalized whole-cell current; V_{I50}, voltage at which the current is half-inactivated; s, slope of the voltage-dependence; τ_1, membrane time constant of inactivation of the first current component.

elicited at a test potential of +80 mV and the mean recovery after washing for 90 s are shown for the various blockers. We tested whether the blockers 4-AP, TEA^+ and quinidine showed a significantly different blocking activity on the K_A and K_D currents and found that the K_A current was blocked significantly more strongly by 10 mmol l^{-1} 4-AP (t-test: $P \leqslant 0.01$) than the K_D current, and that the K_D current was blocked significantly more strongly by 10 mmol l^{-1} TEA^+ (t-test: $P \leqslant 0.01$) than the K_A current, on which it had no significant blocking effect (Wilcoxon's t-test: P=0.01). Quinidine tended to be more effective in blocking the K_D current than the K_A current, but this difference was not statistically significant (t-test: $P \leqslant 0.01$).

Voltage-activated inward currents

In addition to the voltage-activated K^+ currents we have described, we also detected voltage-activated inward currents elicited by the same depolarizing step protocols used to measure the outward currents. These currents became apparent with 10 mmol l^{-1} $BaCl_2$ in the bath and were in the range –90 to –180 pA at 0 mV (measured within the first 30 ms of the depolarizing voltage step). In a further set of recordings, we replaced the internal K^+ by equimolar Cs^+ to exclude contamination of the inward currents by the K^+ outward currents and we increased the external $BaCl_2$ concentration to 20 mmol l^{-1}. Under these conditions, the peak currents increased to 350 pA (Fig. 7A). As shown by the I/V curve (Fig. 7B, determined with 20 mmol l^{-1} $BaCl_2$ in the bath), the current activated at approximately –30 mV and peaked at 0 mV. The current was blocked by 50 µmol l^{-1} Cd^{2+}. This block was partially reversible after a 90 s wash with saline. Since *in vivo* the inward current is probably carried by Ca^{2+}, we determined the peak inward currents with 1 mmol l^{-1} Ca^{2+} in the bath and with Cs^+ replacing the internal K^+. We observed peak inward currents in the range 50–100 pA. The course of the resulting I/V

Table 1. *Summary of the electrophysiological data for the voltage-activated K^+ currents*

	τ_1 (ms)	I_{peak} (nA)		I_{K_A}/I_{K_D} (nA)	V_{G50} (mV)		K_A V_{I50} (mV)	Resting potential (mV)
		K_A	K_D		K_A	K_D		
Group I	12.3±7.9* (21)	8.4±1.9 (21)	0.72±0.23 (22)	12.5±3.5 (21)	–29.9 *s*=11.9 (22)	–20.5 *s*= 20.4 (22)	–84.5 *s*= –6.3 (18)	–37±7.9* (13)
Group II	4.0±3.9* (32)	0.92±0.4 (36)	0.5±0.32 (36)	2.12±1.0 (36)	–7.9 s=26.6 (36)	–7.4 *s*=16.2 (36)	–68.4 *s*= –7.5 (21)	–22.6±6.1* (19)

Values are means ± S.D. Values of *N* are given in parentheses.

An asterisk indicates a statistically significant difference (*t*-test: $P<0.01$).

τ_1, membrane time constant of the first, rapidly inactivating component of the K_A current; I_{peak}, the peak currents of K_A and K_D, respectively, measured at +80 mV; I_{K_A}/I_{K_D}, the ratio of the peak K_A to the peak K_D current of the measured cell; V_{G50}, the voltage of half-activation of the K_A current; *s*, the corresponding slope factor (channel open probability will change e-fold for a change in voltage given by *s*); V_{I50}, the voltage of half-inactivation of the K_A current.

curve in these cells resembles the *I*/*V* curve of the Ba^{2+} currents in Fig. 7A.

Discussion

The results of this study demonstrate that in freshly dissociated somata of lamina neurons voltage-activated membrane currents can be characterized by whole-cell patch-clamp recordings. Measurements on freshly dissociated somata have the advantage that potential artefacts, such as the *de novo* expression of additional Na^+ or Ca^{2+} channels in cultured neurons (Hayashi and Levine, 1992; Schäfer et al., 1994), are excluded. In several cases, it has been shown that voltage-activated currents studied in freshly dissociated somata are unchanged from those measured *in situ* (e.g. Hardie and Weckström, 1990; Benson, 1993; Skingsley et al., 1995).

Whole-cell recordings of freshly dissociated insect neurons were usually performed after enzyme treatment, which may alter the properties of ion channels and receptors (Hardie, 1989; Hardie and Weckström, 1990; Skingsley et al., 1995; Wicher and Penzlin, 1997). In addition, our experiments required a short papain treatment to achieve a reliable and rapid breakthrough into the whole-cell recording mode. In control experiments, without enzyme treatment, we were able to achieve the whole-cell mode after incubation in pure saline at room temperature for approximately 40 min. These recordings revealed no differences in the voltage-activated currents compared with enzyme-treated cells.

Identity of neurons

The lamina is a neuropil composed of homogeneous units, the so-called optic cartridges, each corresponding to a single ommatidium (Kirschfeld, 1973). The lamina consists of a relatively small number of neurons whose somata are located

Table 2. *Summary of the pharmacological data*

Blocker	K_A current (%)	S.D.	*N*	K_D current (%)	S.D.	*N*
10 mmol l^{-1} 4-AP	51.1*	15.1	12	87.1*	15.1	10
Wash	90.5	13.7	8	76.8	18.9	6
10 mmol l^{-1} $BaCl_2$	49.4	11.3	9	51.9	21.5	8
Wash	79.9	22.2	4	54.8	14.6	4
50 µmol l^{-1} quinidine	53.8	17.5	8	20.1	7.6	6
Wash	95.2	22.8	5	65.3	15.6	5
10 mmol l^{-1} TEA^+	95.1*	11.5	19	46.8*	11.6	19
Wash	90.8	17.0	13	68.0	16.1	13
10 mmol l^{-1} CsCl	95.7	23.1	6	74.1	6.8	8

Values for the reduction and recovery of the K_A and the K_D currents are given as a percentage (mean ± S.D.) of the control value (100 %).

An asterisk indicates a statistically significant difference in the effectiveness of a blocker on the K_A and K_D currents (*t*-test: $P<0.01$).

Owing to the small number of cells tested, the data for recovery after external CsCl treatment are not shown.

4-AP, 4-aminopyridine; TEA^+, tetraethylammonium.

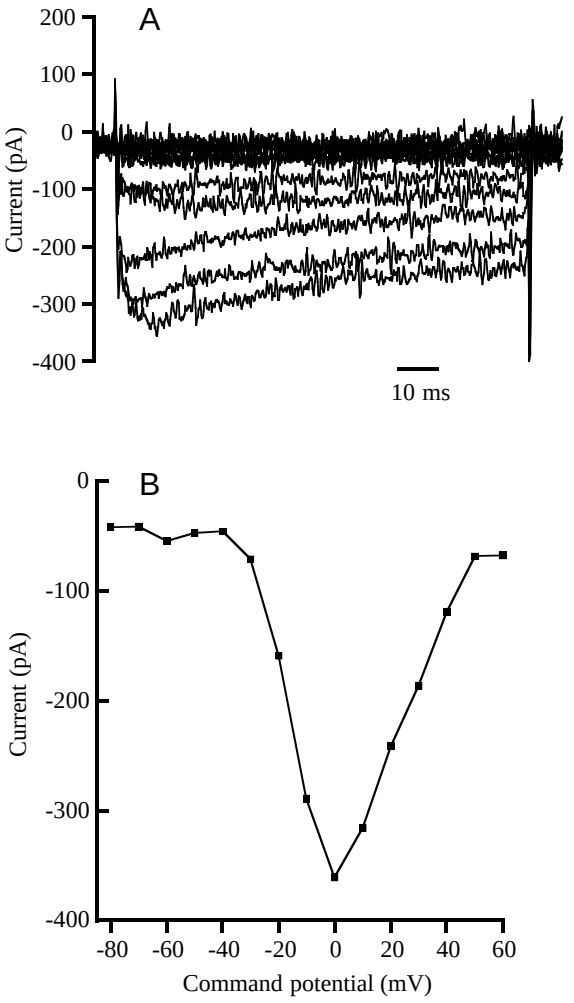

Fig. 7. Voltage-activated inward currents. (A) Inward currents of a locust lamina neuron (evoked by depolarizing voltage steps from –80 mV to +60 mV) were recorded with 20 mmol l^{-1} $BaCl_2$ present in the bath and after replacing internal K^+ by Cs^+. (B) Current/voltage plot of the current shown in A obtained by plotting the peak currents measured within the first 30 ms of the test pulses *versus* the command potential.

in a restricted area distal to the neuropil. The cell bodies of the monopolar cells are located proximal to the basement membrane of the retina. These are columnar neurons with dendritic arborizations in the lamina and an axon that projects to the medulla *via* the first optic chiasma. In *Schistocerca gregaria*, six types of lamina monopolar neurons (M_1–M_6) have been described (Nowel and Shelton, 1981). The axons of the cell types M_1–M_5 project to the proximal and distal layers (with the exception of M_5) of the medulla, and their dendritic arborizations are restricted to one cartridge. Situated more proximally in the lamina are the cell bodies of two types (H1 and H2) of horizontal or amacrine cells (Nowel and Shelton, 1981; Kral, 1987). In dissociating the cell bodies, either by dabbing or using any other method, their processes are disrupted. This leads to the problem of their reliable identification, which is normally achieved on the basis of the morphology of the processes in the neuropil. In a previous study (Schmidt et al., 1998) of recordings from cells dissociated in the same way, we developed criteria allowing a reasonably reliable identification of the recorded somata. Using these criteria, and especially by restricting recordings to somata of 12±1 μm in diameter, it is possible to record mainly, if not exclusively, from lamina monopolar cells.

Voltage-activated currents

All cells recorded in this study supported voltage-activated outward currents. We determined the ionic basis of the outward currents by altering the external and internal ionic milieu. As was to be expected if the observed currents are carried by K^+, inward currents became apparent with increasing $[K^+]_o$ (Fig. 2C). After replacing internal K^+ with equimolar Cs^+, the outward currents were almost completely eliminated. A very small outward current remaining in the presence of internal Cs^+ was also observed in *Drosophila melanogaster* neurons (Wright and Zhong, 1995; Alshuaib and Byerly, 1996). The results of the Cs^+ experiments corroborate our conclusion from the measurement of the reversal potential that the outward currents are carried by K^+, since Cs^+ has a very low relative permeation rate ($\leqslant$0.14; Hille, 1992, p. 352) through K^+ channels.

The voltage-activated outward K^+ currents recorded in the absence of external Ca^{2+} are of two different types. One is a rapidly activating and inactivating transient current whose activation requires a certain period of hyperpolarization to remove inactivation. The second activates more slowly and shows very little or no inactivation during the 100 ms voltage step. Both currents can readily be evoked by depolarizing voltage steps but, in contrast to the transient current, the expression of the late current is not dependent on the previous removal of inactivation. This difference allowed us largely to separate transient from late currents using different voltage-step protocols.

The transient and the late currents can be clearly distinguished by the voltage-dependence of activation and inactivation and by their different sensitivity to 4-AP and TEA^+, blockers known for their specificity. The statistically significant block by 4-AP (compared with the sensitivity to TEA^+), the time course of activation, the short time constant of inactivation τ_1 (Rudy, 1988) and the very negative voltage operating range (Skingsley et al., 1995) identify the transient current in the lamina neurons as a K_A current. K_A currents with very similar properties are expressed in various types of insect neuron (e.g. Solc and Aldrich, 1988; Laurent, 1991; Hayashi and Levine, 1992; Mercer et al., 1995; Schäfer et al., 1994; Grolleau and Lapied, 1995; Wright and Zhong, 1995; Kloppenburg and Hörner, 1998), among them the large monopolar neurons of flies (Skingsley et al., 1995).

The late current, in contrast, with its significant susceptibility to TEA^+, displays kinetic properties of activation and inactivation in common with a more positive voltage operating range (though still at negative voltages). This is

consistent with the so-called delayed-rectifier current (for a review, see Rudy, 1988; Hille, 1992). In accordance with Solc and Aldrich (1988), Hardie and Weckström (1990) and Skingsley et al. (1995), we have called this current the K_D current. The K_D current of locust lamina neurons shares many characteristics with the delayed-rectifier currents observed in neurons of *Manduca sexta* (Hayashi and Levine, 1992; Zufall et al., 1991), *Drosophila melanogaster* (Solc and Aldrich, 1988; Byerly and Leung, 1988), crickets (Kloppenburg and Hörner, 1998; Cayre et al., 1998), *Apis mellifera* (Schäfer et al., 1994) and *Schistocerca gregaria* (Laurent, 1991).

We noticed distinct differences in the properties of the voltage-activated currents of lamina neurons, indicating that the recorded cells do not represent a homogeneous cell type. Most noticeable were differences in the threshold of activation, in the K_A/K_D ratio and in the decay of the fast inactivating current component of K_A. With cluster analysis and subsequently checking the probability of cells belonging to a given group (with regard to nine different variables), we could statistically corroborate that 58 of the recorded cells belonged to one of two groups. Cells with a probability below 0.85 were excluded from the groupwise analysis.

The presence of more than one type of cell differing in their membrane properties is not surprising since it corresponds well to morphological data indicating the existence of six different types (M_1–M_6) of LMCs in the locust lamina (Nowel and Shelton, 1981; Kral, 1987). Our results suggest that the LMCs of locusts differ not only in terms of morphology but also in the expression of various K^+ currents.

K_A and K_D currents in neurons of groups I and II

The cells in groups I and II are mainly distinguished by their voltage-activated K_A currents. In cells of group I, the threshold of activation and the time course of inactivation of K_A are similar to those of the transient current observed in thoracic neurons of *Schistocerca gregaria* (Laurent, 1991). The calculated midpoint of activation (V_{G50}=−29.9 mV) is less negative than that of the L1/L2 LMCs of the blowfly (−78 mV; Hardie and Weckström, 1990). Since the mean current amplitude of K_A at maximal depolarization (+80 mV) is 8.4 nA in group I cells, a large error in command potential (approximately 60 mV at +80 mV) will be caused by uncompensated series resistance. Taking this error into account, the true V_{G50} value of K_A current in group I cells will be 20–30 mV more negative than calculated and thus corresponds very well with the V_{G50} of K_A in LMCs in blowflies. The kinetic properties of the K_A current in group I are similar to those of the K_A currents in LMCs of type L1 or L2 in *Calliphora vicina* (Skingsley et al., 1995). The midpoint of inactivation (V_{I50}=−84.5; s=−6.3 mV) is only slightly more positive than values obtained for LMCs of various dipteran species ranging from −91 mV to −111 mV (Skingsley et al., 1995).

In the threshold of activation, the decay of the fast current component and the steepness of the voltage-dependence of inactivation, the K_A current of group II cells is similar to a K^+ current measured in *Drosophila melanogaster* myotubes (Solc et al., 1987) and overlaps with the type 2 current of *Drosophila melanogaster* Kenyon cells (Wright and Zhong, 1995). The non-inactivating component of the steady-state inactivation curve is presumably due to the intrinsic properties of the K_A channels of cells of group II, since we subtracted the late K_D current from the total current. However, despite the significant differences between the two groups, regarding τ_1 for the peak K_A currents and the steady-state inactivation of K_A, one should remember that this study is based on whole-cell data. This implies certain restrictions: whole-cell currents are probably mediated by the combined action of diverse channel types in which the number of open and closed states can vary (Sontheimer, 1995). The maximal K_A current in group II cells was only 0.92 nA in these measurements, the remaining voltage error being negligible.

The K_D currents of group I and group II cells differ little in terms of activation and whole-cell conductance. The only noticeable difference is a more negative V_{G50} value for group I compared with group II cells. We conclude, therefore, that the underlying K_D channels of both cell types are either identical or very similar. The small differences observed between the two K_D currents could, for instance, be explained by a different combination of K^+ channel subunits (Kamb et al., 1988; Pongs et al., 1988).

Since we have recorded from dissociated cell bodies, it is difficult to estimate the physiological role of the voltage-activated K^+ currents. Nevertheless, it has been shown in LMCs of flies (Guy and Srinivasan, 1988; Weckström et al., 1989; Uusitalo et al., 1995) that light flashes induce transient hyperpolarizations, presumably in response to histamine release from the photoreceptors, followed by transient depolarizations mediated by a voltage-activated Na^+ current. The K_A current in group I cells requires hyperpolarizing voltages to remove inactivation. The histamine-activated Cl^- conductance may partly remove the inactivation of the K_A current. If there is an additional fast Na^+ current, responsible for the off-spike elicited by light pulses, the K_A current may act antagonistically to a depolarizing transient elicited by a light-off stimulus, as observed in *Eristalis tenax* (Guy and Srinivasan, 1988).

Pharmacology of K_A and K_D currents

As previously mentioned, we separated the K_A and K_D currents of the locust lamina neurons electrophysiologically. To test the validity of this separation, we employed blockers that are known to affect K_A and K_D currents selectively. In this respect, especially the statistically significant blocking effect of 4-AP on the K_A current and of TEA^+ on the K_D current of the lamina neurons, the results corroborated the electrophysiological separation (Table 1). In all but one insect neuron type tested, 4-AP has been found to block K_A currents specifically, whereas TEA^+ mainly blocked the K_D currents (Solc and Aldrich, 1988; Laurent, 1991; Hayashi and Levine, 1992; Mercer et al., 1995; Schäfer et al., 1994; Grolleau and Lapied, 1995; Wright and Zhong, 1995; Kloppenburg and

Hörner, 1998). The exception is the type 1 current in *Drosophila melanogaster* mushroom body neurons, which appears to be a K_A current that is virtually insensitive to 4-AP (Wright and Zhong, 1995). As far as we know, the K_A current in lamina neurons of *Schistocerca gregaria* is the only K_A current in insect neurons that is unaffected by TEA^+. This is in contrast to findings in other insect neurons (e.g. Solc and Aldrich, 1988; Byerly and Leung, 1988; Cayre et al., 1998). The second blocker that affected the K_D current was quinidine, but this also reduced the K_A current somewhat. This is consistent with observations in *Drosophila melanogaster* muscle fibres (Singh and Wu, 1989), Kenyon cells of honeybees (Schäfer et al., 1994) and giant interneurons of crickets (Kloppenburg and Hörner, 1998).

Voltage-activated inward currents

In addition to the outward currents carried by K^+ described so far, some cells showed a small inward current with 10 mmol l^{-1} $BaCl_2$ in the bath, which was enhanced at 20 mmol l^{-1} external $BaCl_2$. Its sensitivity to 50 μmol l^{-1} Cd^{2+} and the characteristic shape of the *I*/*V* curve were similar to those of the voltage-activated Ca^{2+}/Ba^{2+} currents recorded in Kenyon cells of the honeybee (Schäfer et al., 1994), in motoneurons of *Manduca sexta* (Hayashi and Levine, 1992), in pars intercerebralis neurons of locusts (Bickmeyer et al., 1994; Pearson et al., 1993) and in the CNS neurons of cockroaches (Christensen et al., 1988; Wicher and Penzlin, 1997). Thus, we assume that in lamina neurons the inward current is also carried by Ca^{2+}, although we did not investigate its ionic basis. Voltage-activated Ca^{2+} channels could mediate the activation of K_{Ca} currents and/or bestow active membrane properties to the cells.

This study was supported by the Deutsche Forschungsgemeinschaft (Ge 249/16-2). We thank Dipl. Biol. Andreas Krüger for help with the cluster analysis and Dr Jochen Röper, Dipl. Biol. Ralf Bruns and Dipl. Biol. Jakob Wolfart for valuable advice regarding the fitting of our data. This article is based on a doctoral study by Dipl. Biol. Christian Benkenstein in the faculty of Biology, University of Hamburg, Germany.

References

Alshuaib, W. B. and Byerly, L. (1996). Modulation of membrane currents by cyclic AMP in cleavage-arrested *Drosophila* neurons. *J. Exp. Biol.* **199**, 537–548.

Bacon, J. P., Thompson, K. S. J. and Stern, M. (1995). Identified octopaminergic neurons provide an arousal mechanism in the locust brain. *J. Neurophysiol.* **74**, 2739–2743.

Benson, J. A. (1993). The electrophysiological pharmacology of neurotransmitter receptors on locust neuronal somata. In *Comparative Molecular Neurobiology* (ed. Y. Pichon), pp. 390–413. Basel: Birkhäuser Verlag.

Bickmeyer, U., Rössler, W. and Wiegand, H. (1994). Calcium channel currents in cultured pars intercerebralis neurosecretory cells of adult *Locusta migratoria*. *J. Exp. Biol.* **197**, 393–398.

Byerly, L. and Leung, H.-T. (1988). Ionic currents of *Drosophila* neurons in embryonic cultures. *J. Neurosci.* **8**, 4379–4393.

Cayre, M., Buckingham, S. D., Strambi, A., Strambi, C. and Sattelle, D. B. (1998). Adult insect mushroom body neurons in primary culture: Cell morphology and characterization of potassium channels. *Cell Tissue Res.* **291**, 537–547.

Christensen, B. N., Larmet, Y., Shimahara, T., Beadle, D. and Pichon, Y. (1988). Ionic currents in neurons cultured from embryonic cockroach (*Periplaneta americana*) brains. *J. Exp. Biol.* **135**, 193–214.

Gewecke, M. and Hou, T. (1993). Visual brain neurons in *Locusta migratoria*. In *Sensory Systems of Arthropods* (ed. K. Wiese), pp. 119–144. Basel: Birkhäuser Verlag.

Grolleau, F. and Lapied, B. (1995). Separation and identification of multiple potassium currents regulating the pacemaker activity of insect neurosecretory cells (DUM neurons). *J. Neurophysiol.* **73**, 160–171.

Guy, R. G. and Srinivasan, M. V. (1998). Integrative properties of second-order visual neurons: A study of large monopolar cells in the dronefly *Eristalis*. *J. Comp. Physiol.* A **162**, 317–331.

Hamill, O. P., Marty, A., Neher, E., Sakman, B. and Sigworth, R. F. (1981). Improved patch-clamp techniques for high resolution current recording from cell-free membrane patches. *Pflügers Arch.* **391**, 85–100.

Hardie, R. C. (1987). Is histamine the neurotransmitter in insect photoreceptors? *J. Comp. Physiol.* A **161**, 201–213.

Hardie, R. C. (1988). Effects of antagonists on putative histamine receptors in the first visual neuropile of the housefly (*Musca domestica*). *J. Exp. Biol.* **138**, 221–241.

Hardie, R. C. (1989). A histamine-activated chloride channel involved in neurotransmission at a photoreceptor synapse. *Nature* **339**, 704–706.

Hardie, R. C. and Weckström, M. (1990). Three classes of potassium channels in large monopolar cells of the blowfly *Calliphora vicina*. *J. Comp. Physiol.* A **167**, 723–736.

Hayashi, J. H. and Levine, R. B. (1992). Calcium and potassium currents in leg motoneurons during postembryonic development in the hawkmoth *Manduca sexta*. *J. Exp. Biol.* **171**, 15–42.

Hevers, W. and Hardie, R. C. (1995). Serotonin modulates the voltage dependence of delayed rectifier and *Shaker* potassium channels in *Drosophila* photoreceptors. *Neuron* **14**, 845–856.

Hille, B. (1992). *Ionic Channels of Excitable Membranes*, second edition. Sunderland, MA: Sinauer Associates Inc.

Homberg, U. (1994). *Distribution of Neurotransmitters in the Insect Brain.* Progress in Zoology series, Fischer Verlag.

Kamb, A., Tseng-Crank, J. and Tanouye, M. A. (1988). Multiple products of the *Drosophila Shaker* gene contribute to potassium channel diversity. *Neuron* **1**, 421–430.

Kirschfeld, K. (1973). Das neurale Superpositionsauge. *Fortschr. Zool.* **21**, 229–257.

Kloppenburg, P. and Hörner, M. (1998). Voltage-activated currents in identified giant interneurones isolated from adult crickets *Gryllus bimaculatus*. *J. Exp. Biol.* **201**, 2529–2541.

Kral, K. (1987). Organization of the first optic neuropil (or lamina) in different insect species. In *Arthropod Brain* (ed. A. P. Gupta), pp. 181–201. New York: John Wiley & Sons.

Laurent, G. (1991). Evidence for voltage-activated outward currents in the neuropilar membrane of locust nonspiking local interneurons. *J. Neurosci.* **11**, 1713–1726.

Mercer, A. R., Hayashi, J. H. and Hildebrand, J. G. (1995). Modulatory effects of 5-hydroxytryptamine on voltage-activated

currents in cultured antennal lobe neurones of the sphinx moth *Manduca sexta*. *J. Exp. Biol.* **198**, 613–627.

Mittman, S., Flaming, D. G., Copenhagen, D. R. and Belgum, J. H. (1987). Bubble pressure measurement of micropipet tip outer diameter. *J. Neurosci. Meth.* **22**, 161–166.

Nässel, D. R. (1991). Neurotransmitters and neuromodulators in the insect visual system. *Prog. Neurobiol.* **37**, 179–254.

Neher, E. (1992). Correction for liquid junction potentials in patch clamp experiments. *Meth. Enzymol.* **207**, 123–131.

Nowel, M. S. and Shelton, P. M. J. (1981). A Golgi-electron-microscopical study of the structure and development of the lamina ganglionaris of the locust optic lobe. *Cell Tissue Res.* **216**, 377–401.

O'Shea, M., Rowell, C. H. F. and Williams, J. L. D. (1974). The anatomy of a locust visual interneurone; the descending contralateral movement detector. *J. Exp. Biol.* **60**, 1–12.

Pearson, H. A., Lees, G. and Wray, D. (1993). Calcium channel currents in neurones from locust (*Schistocerca gregaria*) thoracic ganglia. *J. Exp. Biol.* **177**, 201–221.

Pongs, O, Kecskemethy, N., Müller, R., Krah-Jentgens, I., Baumann, A., Kiltz, H. H., Canal, I., Llamazares, S., Farrus, A. (1988). *Shaker* encodes a family of putative potassium channel proteins in the nervous system of *Drosophila*. *EMBO J.* **7**, 1087–1096.

Rind, F. C. (1990a). A directionally selective motion-detective neurone in the brain of the locust: physiological and morphological characterization. *J. Exp. Biol.* **149**, 1–19.

Rind, F. C. (1990b). Identification of directionally selective motion-detective neurones in the locust lobula and their synaptic connections with an identified descending neurone. *J. Exp. Biol.* **149**, 21–43.

Rudy, B. (1988). Diversity and ubiquity of K channels. *Neurosci.* **25**, 729–749.

Schäfer, S., Rosenboom, H. and Menzel, R. (1994). Ionic currents of Kenyon cells from the mushroom body of the honeybee. *J. Neurosci.* **14**, 4600–4612.

Schmidt, M., Benkenstein, C. and Gewecke, M. (1998). Patch-clamp analysis of voltage- and ligand-activated whole-cell currents in freshly dissociated neurons of the locust optic lobe. *J. Comp. Physiol.* A **182**, 677–686.

Singh, S. and Wu, C.-F. (1989). Complete separation of four potassium currents in *Drosophila*. *Neuron* **2**, 1325–1329.

Skingsley, D. R., Laughlin, S. B. and Hardie, R. C. (1995). Properties of histamine-activated channels in the large monopolar cells of the dipteran compound eye: a comparative study. *J. Comp. Physiol.* A **176**, 611–623.

Solc, C. K. and Aldrich, R. W. (1988). Voltage-gated potassium channels in larval CNS neurons of *Drosophila*. *J. Neurosci.* **8**, 2256–2570.

Solc, C. K., Zagotta, W. N. and Aldrich, R. W. (1987). Single-channel and genetic analyses reveal two distinct A-type potassium channels in *Drosophila*. *Science* **236**, 1094–1098.

Sontheimer, H. (1995). Whole-cell patch-clamp recordings. In *Patch-Clamp Application and Protocols* (ed. A. A. Boulton, G. B. Baker and W. Walz), pp. 63–64. Totowa, NJ: Humana Press

Stavenga, D. G. and Hardie, R. C. (1989). (eds) *Facets of Vision*. Berlin, Heidelberg: Springer Verlag.

Stern, M., Thompson, K. S. J., Zhou, P., Watson, D. G., Midgley, J. M., Gewecke, M. and Bacon, J. P. (1995). Octopaminergic neurons in the locust brain: Morphological, biochemical and electrophysiological characterisation of potential modulators of the visual system. *J. Comp. Physiol.* A **177**, 611–625.

Uusitalo, R. O., Juusola, M. and Weckström, M. (1995). Graded responses and spiking properties of identified first-order visual interneurones of the fly compound eye. *J. Neurophysiol.* **73**, 1782–1792.

Weckström, M., Kouvalainen, E. and Djupsund, K. (1989). More than one type of conductance is activated during responses of blowfly monopolar neurones. *J. Exp. Biol.* **144**, 147–154.

Wicher, D. and Penzlin, H. (1997). Ca^{2+} currents in central insect neurons: Electrophysiological and pharmacological properties. *J. Neurophysiol.* **77**, 186–199.

Wright, N. J. D. and Zhong, Y. (1995). Characterization of K^+ currents and the cyclic AMP-dependent modulation in cultured *Drosophila* mushroom body neurons identified by *lacZ* expression. *J. Neurosci.* **15**, 1025–1034.

Zufall, F., Stengl, M., Franke, C., Hildebrand, J. G. and Hatt, H. (1991). Ionic currents of cultured olfactory receptor neurons from antennae of male *Manduca sexta*. *J. Neurosci.* **11**, 956–965.